

1 **VolcAshDB – A global database of volcanic ash particles**

2 Damia Benet<sup>1\*</sup>, Fidel Costa<sup>1,2,3</sup>, Kevin Migadel<sup>1</sup>, Daniel W. J. Lee<sup>4</sup>, Claudia D’Oriano<sup>5</sup>, Massimo  
3 Pompilio<sup>5</sup>, Dini Nurfiani<sup>6</sup>, Hamdi Rifai<sup>7</sup>

4  
5 1: Institut de Physique du Globe de Paris, Université Paris Cité, Paris, France

6 2: Earth Observatory of Singapore, Nanyang Technological University, Singapore

7 3: Asian School of the Environment, Nanyang Technological University, Singapore

8 4: Lamont-Doherty Earth Observatory, Columbia University, New York, NY, USA

9 5: Istituto Nazionale di Geofisica e Vulcanologia, sezione di Pisa, Pisa, Italy

10 6: National Research and Innovation Agency (BRIN), Bandung, Indonesia

11 7: Physics Department, Faculty of Mathematics and Natural Sciences, Universitas Negeri Padang,  
12 Indonesia

13 \*Corresponding author(s): Damia Benet ([dbenet@ipgp.fr](mailto:dbenet@ipgp.fr))

14  
15  
16  
17  
18 **This manuscript hasn’t been peer-reviewed and is currently in review in**  
19 ***Scientific Data***

20

## 21 **Abstract** (*Maximum 170 words recommended*)

22 Volcanic ash is made of particles smaller than 2 mm and is produced during volcanic eruptions.  
23 Studying the properties of volcanic ash is key for a range of applications, including volcano monitoring.  
24 However, given the large variety of textures, colors, and shapes of particles from different eruptions  
25 and volcanoes it is challenging to classify them in a reproducible and systematic manner. Here, we  
26 present an open access web-based platform that displays the contents of a database of volcanic ash  
27 particles, VolcAshDB (<https://volcashdb.ipgp.fr/>). Particle data includes optical microscope images,  
28 physical characteristics of the shape, texture and color, and a classification label with the particle type  
29 (free-crystal, altered material, juvenile or lithic). It currently hosts data of 12,044 particles from 53  
30 samples across 13 volcanoes that can be visualized and downloaded in a user-friendly manner. The  
31 database has already been used to develop particle classifiers with Machine Learning. We plan to  
32 continue it to grow and encourage the volcano community to contribute towards standardizing  
33 volcanic ash classification.

## 34

## 35 **Background & Summary**

36 Volcanic ash is made of particles smaller than 2 mm in diameter and is produced during explosive  
37 eruptions. The study of its chemical composition and physical properties is important for a range of  
38 applications, from understanding the impact of volcanic plumes to the Earth's climate<sup>1</sup> or air traffic<sup>2</sup>,  
39 through human health impacts<sup>3</sup> as well as to monitoring the beginning and end of an eruption, and  
40 transition among eruptive styles<sup>4-7</sup>. In particular for monitoring purposes, using volcanic ash requires  
41 the proper identification and characterization of its particles into different components (free crystals,  
42 altered material, lithic, and juvenile). However, it is commonly difficult to unequivocally associate the  
43 features observed under the optical and scanning electron microscopes to a given particle type<sup>8</sup>.  
44 Moreover, the criteria for classification and measurement of particle characteristics are not  
45 standardized, and thus, the volcanic ash particle data are hard to compare between different  
46 eruptions and volcanoes.

47  
48 To alleviate this situation, Benet et al.<sup>9</sup> created the Volcanic Ash DataBase (VolcAshDB) which aims at  
49 compiling the physical and visual characteristics of ash particles from a range of eruptions and  
50 volcanoes using a standardized methodology. As of now, data of 12,044 ash particles from 25  
51 eruptions across 13 volcanoes (Figure 1A) have been collected. The dataset was used to develop  
52 Machine Learning (ML)-based models that are able to automatically classify volcanic ash particles into  
53 different categories<sup>10</sup> and thus opens opportunities for comparative studies between eruptions and  
54 for time-series analysis that could be used during volcanic crises. Here, we present the database  
55 design, web interface (<https://volcashdb.ipgp.fr/>), and resources to download, navigate and visualize  
56 the database contents. Our plan is to continue to grow the database to increase its robustness and  
57 representativity of the wide ranges of volcanic ash, and to encourage the volcano community to  
58 contribute to VolcAshDB to advance towards standardising volcanic ash particle classification.

## 59

## 60 **Methods**

61 **Procedure for image acquisition of ash particles.** Samples were first ultrasonically cleaned, dried and  
62 sieved using four meshes of  $0\phi$  (1 mm),  $1\phi$  (0.5 mm),  $2\phi$  (0.25 mm), and  $3\phi$  (0.125 mm) pore-size  
63 dimensions. Using the coarsest available grain-size per sample, particles were arranged on adhesive-  
64 coated glass slides for scanning on a binocular scanning stage. Several scans at different focal depths  
65 were obtained and “fused” into a 2D-array with a good particle focus. The resulting scans were  
66 segmented and color normalized to generate individual, high-resolution ( $\sim 1,800$  pixels/mm in  
67 average) particle images that are the main data type of the dataset (see more details in Benet et al.<sup>9</sup>).  
68 The images were obtained using a Leica binocular microscope equipped with an LMT260 XY Scanning  
69 Stage and a LAS X imaging software at Nanyang Technological University, Singapore (Benet et al.<sup>9</sup>),  
70 and a binocular scanning stage, Keyence VHX-7000, coupled with its Keyence machine system and  
71 software at Institut de Physique du Globe de Paris (IPGP).

72

73 **Extraction of features from images of particles.** Particle images were quantitatively analyzed to  
74 extract 33 measurements of particle properties (Figure 1B), hereafter called features. These  
75 characterize the particle shape, texture, and color (see Figure 1C for three examples; and Benet et al.<sup>9</sup>  
76 for their definition and calculation). Shape features were obtained from the particle contour and have  
77 been extensively used to characterize perimeter-based irregularities, particle-scale cavities, and/or  
78 overall external morphology<sup>11-13</sup>. Textural features were quantified from the distribution of grayscale  
79 pixel intensity values on the particle surface. Features such as the dissimilarity or correlation are  
80 calculated from the Gray Level Co-occurrence Matrix (GLCM<sup>14</sup>), to distinguish for example between  
81 high textural complexity and uniform smoothness. Color features were extracted as the mean, mode  
82 and standard deviation of the distribution of each channel in both the Red-Green-Blue (RGB) and Hue-  
83 Saturation-Value (HSV) color spaces. These features are sensitive to chromaticity, indicative of  
84 dominant color hues, intensity, and brightness. The procedure for feature extraction was automated  
85 through a Python script available in a public GitHub repository ([https://github.com/dbenet-](https://github.com/dbenet-max/volcashdb_classification)  
86 [max/volcashdb\\_classification](https://github.com/dbenet-max/volcashdb_classification)) and run in the High-Performance Computing center S-CAPAD at IPGP.  
87

88 **Procedure for image classification.** Ash particles were classified from visual inspection of the images  
89 into free-crystal, altered material, juvenile and lithic types (Figure 1C) following the criteria described  
90 in<sup>9</sup>. The main approach involves recognizing diagnostic features for each type. In short: Free crystals  
91 are identified by their well-faceted shapes, sometimes exhibiting twinning and cleavage, and color.  
92 Altered material appears in colors ranging from white to yellowish, with a granular texture and a  
93 variety of hydrothermal secondary minerals, sometimes showing devitrification textures and  
94 secondary minerals. Lithic particles are characterized by their dark, dull appearance, and non-vesicular  
95 density with incipient alteration and rounded edges. The classification of some of the particles  
96 sometimes included Scanning Electron Microscope (SEM) analysis to examine for etch pits or  
97 alteration signs. Juvenile particles are distinguished by their gloss, smooth-skinned surface and lack of  
98 alteration. SEM analyses are sometimes necessary to ascertain the lack of alteration signs<sup>6,15,16</sup>.  
99

100 **Database design.** The database is structured using MongoDB, a NoSQL database that organizes data  
101 into flexible, schema-less *collections*. These *collections* store and manage various types of volcanic  
102 data (Table 1). They include the *Volcanoes* and *Eruptions* *collections* (Figure 2) which record basic  
103 information such as the vent location, eruption date, main rock compositions, and are sourced from  
104 Smithsonian's "Volcanoes of the World" database<sup>17</sup>. The *Ash-Forming Events (AFEs) collection* records  
105 information about the ash-forming event such as the date and its volcanic context (e.g., eruptive style).  
106 The *Samples collection* contains information about sampling details such as the location and  
107 technique, and lab procedures such as cleaning and sieving. The *Particles collection* contains a unique  
108 identifier for each particle with its associated image, metadata such as the imaging conditions, and  
109 the 33 measured *features*.  
110

111 **Architecture and Technologies of VolcAshDB web-based platform.** The platform consists of two main  
112 parts, a data input of images from which the features are extracted, and a data output that allows for  
113 search, visualization, analysis and downloading of the data (Figure 3). The platform is built using the  
114 MERN stack, which includes MongoDB, Express.js, React.js, and Node.js. The backend uses Node.js  
115 and Express.js for server-side functions, while MongoDB stores and manages the data. The frontend  
116 is built with React.js, providing a responsive interface for easy interaction and visualization.  
117 Communication between the client and server is handled through a RESTful API. The platform runs on  
118 a Linux server managed by Proxmox VE, with deployment managed by PM2 for process control.  
119

## 120 **Data Records**

121 **Access.** VolcAshDB contents are publicly accessible for image and feature visualization and plotting  
122 through the VolcAshDB interface at <https://volcashdb.ipgp.fr/catalogue>, and for download after

123 logging in. To sign up, users must provide an email for verification. The data are licensed under CC-BY-  
124 4.0 and can be cited using the DOI <https://doi.org/10.18715/ipgp.2024.lx32oxw9>.

125

126 **Data coverage.** As of September 2024, VolcAshDB contains the 33 *features* and classified image data  
127 from 12,044 volcanic ash particles from 53 samples across 13 different volcanoes (Table 2). The  
128 collection comprises basaltic to rhyolitic magmas, and a range of activity types, including phreatic  
129 eruptions, lava dome explosions, basaltic lava fountaining, and Plinian to Sub-Plinian eruptions. The  
130 database also includes experimental samples that provide insights into the effect of alteration of the  
131 particles under a range of specific conditions of temperature and oxygen fugacity<sup>18</sup>. Some of our  
132 samples have also been used to better understand volcanic processes during activity, such as for  
133 Nevados de Chillán eruptive period, 2016-2018<sup>19</sup>, or are currently being investigated to obtain critical  
134 insights into the eruption progression at Marapi, 2023–2024 (Nurfiani et al., *in prep*).

135

## 136 **Technical Validation**

137 **Effect of image resolution and focus on measured features.** To evaluate how the features extracted  
138 from the particle images are affected by poor resolution or focus, we modeled how the feature values  
139 change by varying the two parameters on our particle images. For this we used four particle images  
140 with different shape, texture and color. The resolution unit we use to model is defined by the number  
141 of pixels (pxls) comprised in the area (a) of the particle per image (pxls/a). We found that feature  
142 values only begin to shift when resolution falls below  $3.5 \times 10^4$  pxls/a, whereas our average image  
143 resolution is  $1.41 \times 10^6$  pxls/a, confirming that our resolution is more than sufficient (Figure 4A). To  
144 evaluate the effect of focus, we applied a Gaussian blur to the images (measured in sigmas). We found  
145 that feature values remain stable until the blur reaches 0.2 sigma, beyond which convexity starts to  
146 change and some instances become truncated (Figure 4B). This shows that extracted features in our  
147 database are not influenced by poor focus.

148

## 149 **Usage Notes**

150 **Catalogue, Image Browsing and Data Download.** Users can access the page “Catalogue” at  
151 <https://volcashdb.ipgp.fr/catalogue> to browse images. The catalogue contains two subsets of data,  
152 those of natural samples and those of experimental samples. Users can swap between them by ticking  
153 the “Natural Data” button. Advanced image searching can be done by using a set of filters displayed  
154 as tags with dropdown menus (Figure 5). Filters include options for volcano, eruptive activity type,  
155 grain-size fraction, particle type and shape. To download the filtered images, particle features and  
156 metadata, users must first sign up by providing an email address, country, and institute. Upon email  
157 verification, users will be able to click on “Apply Filters” and “Download Images and Measured  
158 Features”. A zip file is automatically created which can be downloaded with the filtered particle images  
159 and an excel spreadsheet. The spreadsheet contains the particle features and metadata (imaging  
160 conditions, volcano, date of emission, etc.) and each row represents a particle of the dataset.

161

162 **Data analysis and Plots.** Users can access <https://volcashdb.ipgp.fr/analytic> to visualize and interact  
163 with various plots that illustrate the contents of the database in various manners (Figure 6). Plots are  
164 provided for natural or experimental samples, and users can swap between them by ticking the  
165 “Natural Data” button. Pie charts show the proportions of number of particles per volcano, per particle  
166 type and per activity type, and users can select or unselect specific subgroups. Juvenile–Altered  
167 material–Lithic ternary diagrams show the proportion of particle types normalized without free  
168 crystals per sample and according to eruptive activity type. We also analyze by Principal Component  
169 Analysis the features as reported in Benet et al.<sup>9</sup> and show the data transformed into the Principal  
170 Components 1 and 2. The plot is accompanied with a dropdown menu that allows users to select  
171 among eruptive activity types. The “Subplinian”, for instance, shows a distinctive cluster of juvenile  
172 particles in violet color. Histograms show the distribution of values of a given feature and two

173 dropdown menus allow choosing which feature and by which volcano. Further insights from all plots  
174 can be obtained by hovering with the mouse over any marker.

175

### 176 **Code Availability**

177 The Python program for feature extraction and for Principal Component Analysis are available  
178 at <https://github.com/dbenet-ntu/VolcAsh-Project>. The code for the web-based platform is available  
179 at [https://github.com/dbenet-ntu/VolcAshDB-web\\_Sept2024](https://github.com/dbenet-ntu/VolcAshDB-web_Sept2024). The Python code was developed using  
180 its version 3.9. Data wrangling and analysis was done using Numpy v.1.21.6, Pandas v. 1.3.5, image  
181 processing using Scikit-image v.0.19.2 and opencv v.3.4.2, and plotting by matplotlib v.3.5.1 and  
182 seaborn v.0.11.2.

183

### 184 **Acknowledgements**

185 Damia Benet is very grateful to David Weissenbach and Michel Le Cocq for their continued assistance  
186 in setting up the virtual machine and in the deployment of various features of VolcAshDB and to  
187 Christina Widiwijayanti for insightful discussions about the metadata and design of the database. This  
188 research was supported via Fidel Costa's Chaire d'Excellence grant by the Université Paris Cité.

189

### 190 **Author contributions**

191 Benet led the development, acquired and processed the data, and wrote the original manuscript of  
192 the project, which was supervised and revised by Costa. Migadel and Benet led the development of  
193 front-end and the back-end of the web-platform. Lee, D'Oriano, Pompilio, Nurfiani and Rifai provided  
194 some samples. The final version of the manuscript has been read, reviewed and approved by all co-  
195 authors.

196

### 197 **Competing interests**

198 The authors declare no competing interests.

199

200 **Figures**

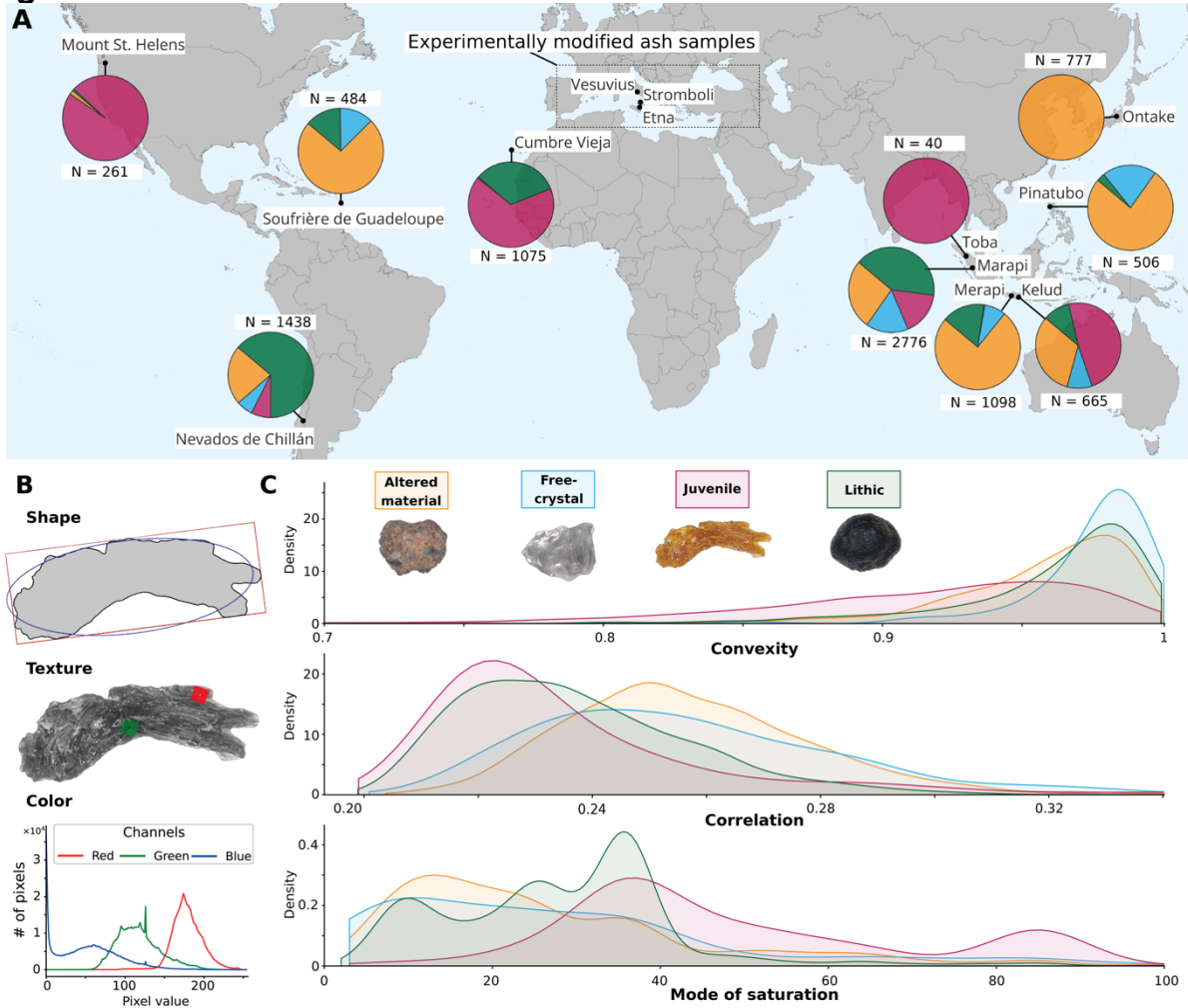


Figure 1

201  
202

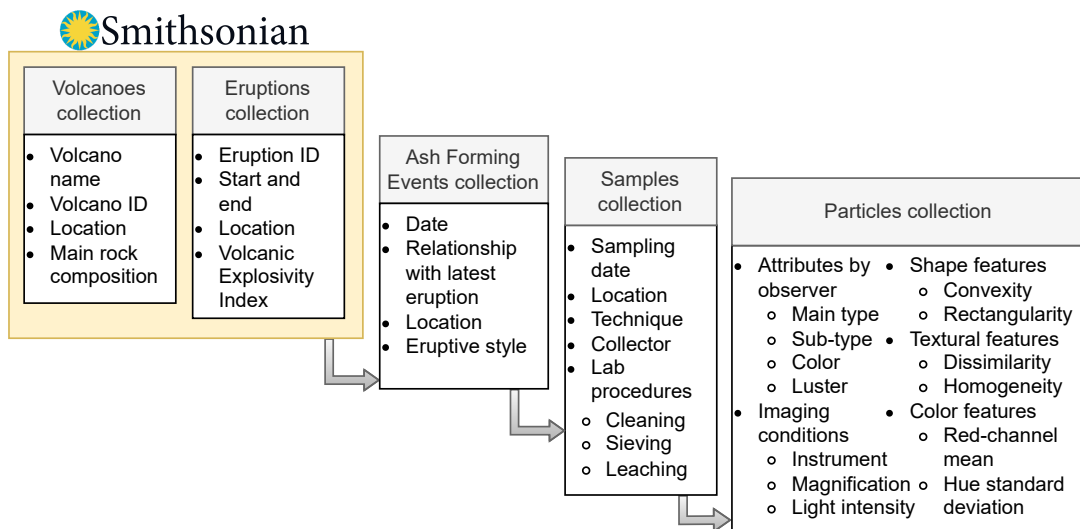


Figure 2

203  
204  
205

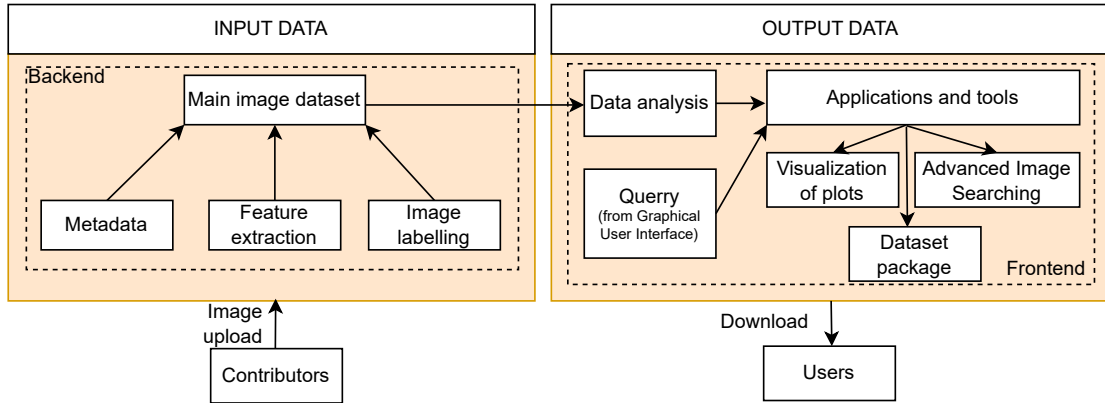


Figure 3

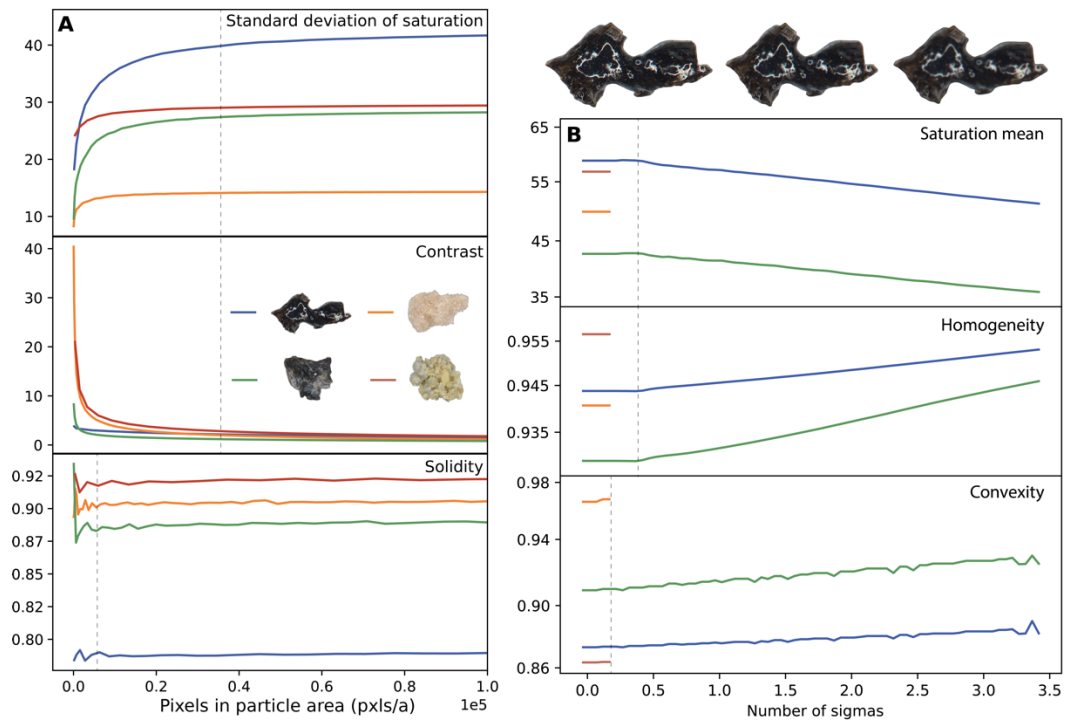


Figure 4

VolcAshDB HOME ABOUT CATALOGUE PLOTS

## Explore the Database

Search by Volcano Name, Particle Type, etc or click the tag(s) below

[La Palma](#)
[Eruptions](#)
[Eruptive Style](#)
[Grain Size](#)
[juvenile](#)
[fluidal](#)
[low crystallinity](#)
[Color](#)
[Hydrothermal Alteration Degree](#)
[juvenile Type](#)
[Lithic Type](#)
[Altered Material Type](#)
[Free Crystal Type](#)

[APPLY FILTERS](#)
[DOWNLOAD IMAGES AND MEASURED FEATURES](#)

356 search results for "La Palma,juvenile,low crystallinity,fluidal":

You can now annotate the particle images by double-clicking on them!

**PARTICLE**

Figure 5

206  
207  
208

209  
210  
211

212  
213  
214

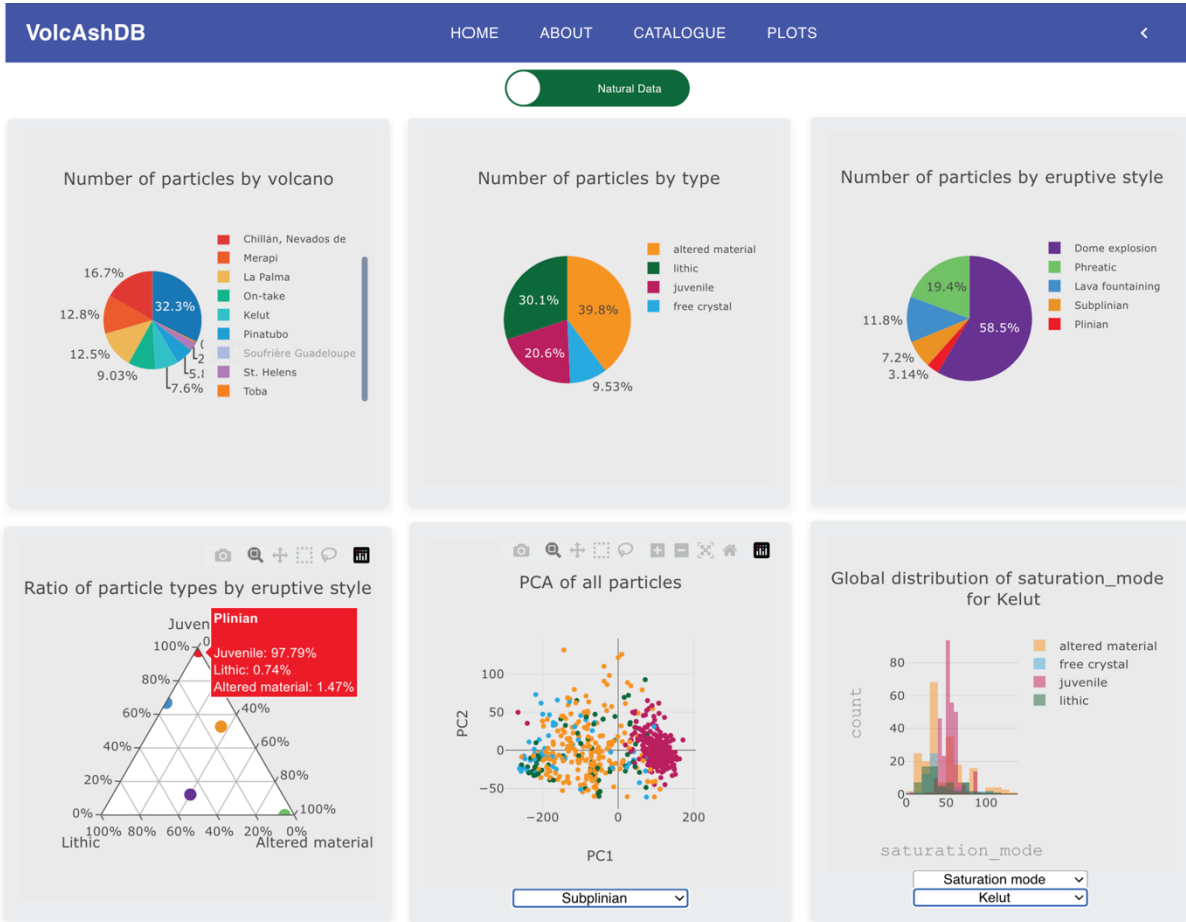


Figure 6

216  
217218 **Figure Legends**

219 Figure 1: Summary of the main contents and data types found in VolcAshDB. (A) World map<sup>20</sup> with the  
 220 location of volcanoes for which we have collected data, and pie charts showing the average proportion  
 221 of the particle main types (orange color is altered material, blue is free-crystal, violet is juvenile and  
 222 green is lithic) of samples by volcano. (B) Examples of the properties we have measured for each ash  
 223 particle, including the contour for shape, the grayscale homogeneity of the surface for texture, and  
 224 the color-channels histogram distributions for color. (C) Plots showing the varied distributions of three  
 225 particle features (convexity, correlation, mode of saturation) across the four main types (color-coded  
 226 as above). "Density", in the y-axis, is the probability density function calculated by the Kernel Density  
 227 Estimate plot, which can take values above 1.

228  
229

230 Figure 2. Schematic of the database hierarchical design based on five MongoDB *collections*. Lists within  
 231 bullet points are not exhaustive. *Volcanoes* and *Eruptions* collections were adopted from  
 232 Smithsonian's "Volcanoes of the World" database (Global Volcanism Program, 2024).

233  
234

Figure 3. Dataflow, main tasks and general architecture of the web-based platform.

235  
236

Figure 4. Plots with the modelled feature values to estimate the influence of image focus and  
 237 resolution. (A) The values of the features standard deviation of saturation, contrast, solidity are  
 238 modelled by decreasing pixel resolution, and (B) the values of saturation mean, homogeneity,  
 239 convexity are modelled at varying blur for four representative particle images with grain-size between  
 240 1–2 mm. Colors of the curves in (A) and (B) correspond to the different particles shown inside the



241 “Contrast” panel. The effect of the Gaussian blur to the original image (top-left image) is shown at 5  
 242 (top-center) and 10 (top-right) sigmas. Dashed lines indicate the values of resolution or focus beyond  
 243 which feature values start to shift.

244

245 Figure 5. Screenshot of the “Catalogue” page in VolcAshDB web site. The screenshot includes the  
 246 following filters: “Volcano Name” as “La Palma”, “Main Type” as “juvenile”, “Shape” as “fluidal” and  
 247 “Crystallinity” as “low”. The white bars show the scale for 1 mm under the microscope.

248

249 Figure 6. Screenshots of six representative plots from the “Plots” page in VolcAshDB web site.

250

## 251 Tables

252 Table 1: List of fields and definitions of the collections that make VolcAshDB.

Field	Type	Optionality	Description
<i>Volcanoes collection (source Smithsonian database)</i>			
_id	ObjectId	O <sup>1</sup>	Document identifier
volc_name	String	M <sup>2</sup>	Volcano name
volc_num	Int(32)	M	Volcano identifier
volc_slat	String	M	Volcano location (latitude)
volc_slon	String	M	Volcano location (longitude)
volc_status	String	O	Status of the volcano
volc_type	String	O	Type of volcano
<i>Eruptions collection (source Smithsonian database)</i>			
_id	ObjectId	O	Document identifier
volc_num	Int(32)	M	Volcano identifier
volc_name	String	M	Volcano name
ed_stime	Date	M	Eruption start date
ed_etime	Date	M	Eruption end date
<i>Ash-Forming Events collection</i>			
_id	ObjectId	O	Document identifier
afe_code	String	M	Ash forming event identifier
volc_num	Int(32)	M	Volcano identifier
afe_date	Date	M	Ash forming event date
eruptive_style	String	M	Description of eruption style
afe_lat	String	M	Ash forming event location (latitude)
afe_lon	String	M	Ash forming event location (longitude)
plume_col	String	O	Plume color
max_plume_height	Int(32)	O	Maximum recorded plume height
fumarolic_activity	String	O	Observed fumarolic activity intensity
<i>Samples collection</i>			
_id	ObjectId	O	Document identifier
sample_stime	Date	M	Sampling date
sample_lat	String	M	Sampling coordinate latitude
sample_lon	String	M	Sampling coordinate longitude

sample_nat	Boolean	M	Sample is natural or experimental
sample_techn	String	O	Technique (e.g. ashmeter)
sample_surf	String	O	Sampling surface (e.g. roof)
sample_collector	String	O	Collector/s name
ultrasound	Boolean	O	Ultrasonicated
gsLow	String	M	Lower value of grain-size fraction
gsUp	String	M	Upper value of grain-size fraction
<i>Particles collection</i>			
_id	ObjectId	O	Document identifier
imgURL	String	M	Filename of the particle's image
main_type	Object	M	Main type of the particle
sub_type	String	O	Sub type of the particle
color	String	O	Color of the particle
luster	String	O	Luster of the particle
shape	String	O	Shape of the particle
crystallinity	String	O	Crystallinity of the particle
alter_degree	String	O	Degree of alteration of the particle
weathering_sign	String	O	Presence of weathering signs
instrument	String	O	Instrument for particle image
magnification	Int(32)	O	Magnification of particle image
multi_focus	Boolean	O	Use of multi-focus for particle image
convexity <sup>3</sup>	Double	M	Convexity of the particle (shape)
contrast <sup>3</sup>	Double	M	Contrast of the particle (texture)
hue_mean <sup>3</sup>	Double	M	Mean value of hue histogram (color)

253 1: "O" stands for "Optional"

254 2: "M" stands for "Mandatory"

255 3: Only one feature for each category of shape, texture and color is listed as example. See Benet et al  
256 <sup>9</sup> for more details.

257

258 Table 2: Characteristics of the volcanoes represented in our database and number of particles that  
259 have been analyzed and archived.

Volcano	Magma composition	Volcano type	Reference	# particle images
Cumbre Vieja	Trachybasalt / Tephrite Basanite	Cinder cone	<sup>21</sup>	1075
Kelud	Andesite / Basaltic Andesite	Stratovolcano	<sup>22</sup>	665
Merapi	Basaltic Andesite	Stratovolcano	<sup>23</sup>	1098
Soufrière de Guadeloupe	Basaltic andesite- Andesite	Stratovolcano	<sup>24</sup>	484
Nevados de Chillán	Basaltic-Andesite	Dome complex	<sup>25</sup>	1438
Ontake	Andesite	Stratovolcano	<sup>26</sup>	777
Pinatubo	Dacite	Caldera	<sup>27</sup>	506

Mount St. Helens	Dacite	Stratovolcano	28	261
Marapi	Andesite	Stratovolcano	29	2776
Toba	Dacite / Rhyolite	Caldera	30	40
Vesuvius (EXP) <sup>1</sup>	Tephriphonolite	Stratovolcano	18	806
Etna (EXP)	Trachybasalt / Tephrite Basanite	Stratovolcano	18	1374
Stromboli (EXP)	Basalt	Stratovolcano	18	645

260 1: (EXP) denotes that the sample has been experimentally obtained for example by crushing  
261 scoria into ash-sized grains <sup>18</sup>.

262

## 263 References

- 264 1. Self, S. Effects of volcanic eruptions on the atmosphere and climate. in (eds. Joan Martí &  
265 Gerald G. J. Ernst) (Cambridge: Cambridge University Press, 2005).
- 266 2. Bonadonna, C., Biass, S., Menoni, S. & Gregg, C. E. Assessment of risk associated with tephra-  
267 related hazards. in *Forecasting and Planning for Volcanic Hazards, Risks, and Disasters* 329–  
268 378 (Elsevier, 2020). doi:10.1016/B978-0-12-818082-2.00008-1.
- 269 3. Horwell, C. J. *et al.* A physico-chemical assessment of the health hazard of Mt. Vesuvius volcanic  
270 ash. *Journal of Volcanology and Geothermal Research* **191**, 222–232 (2010).
- 271 4. Miwa, T., Geshi, N. & Shinohara, H. Temporal variation in volcanic ash texture during a  
272 vulcanian eruption at the sakurajima volcano, Japan. *Journal of Volcanology and Geothermal*  
273 *Research* **260**, 80–89 (2013).
- 274 5. Suzuki, Y. *et al.* Precursory activity and evolution of the 2011 eruption of Shinmoe-dake in  
275 Kirishima volcano—insights from ash samples. *Earth, Planets and Space* **65**, 591–607 (2013).
- 276 6. Gaunt, H. E. *et al.* Juvenile magma recognition and eruptive dynamics inferred from the analysis  
277 of ash time series: The 2015 reawakening of Cotopaxi volcano. *Journal of Volcanology and*  
278 *Geothermal Research* **328**, 134–146 (2016).
- 279 7. Cashman, K. V. & Hoblitt, R. P. Magmatic precursors to the 18 May 1980 eruption of Mount St.  
280 Helens, USA. *Geology* **32**, 141–144 (2004).
- 281 8. Pardo, N. *et al.* Perils in distinguishing phreatic from phreatomagmatic ash; insights into the  
282 eruption mechanisms of the 6 August 2012 Mt. Tongariro eruption, New Zealand. *Journal of*  
283 *Volcanology and Geothermal Research* **286**, 397–414 (2014).
- 284 9. Benet, D. *et al.* VolcAshDB: a Volcanic Ash DataBase of classified particle images and features.  
285 *Bull Volcanol* **86**, (2024).
- 286 10. Benet, D., Costa, F. & Widiwijayanti, C. Volcanic Ash Classification Through Machine Learning.  
287 *Geochemistry, Geophysics, Geosystems* **25**, (2024).
- 288 11. Liu, E. J., Cashman, K. V. & Rust, A. C. Optimising shape analysis to quantify volcanic ash  
289 morphology. *GeoResJ* **8**, 14–30 (2015).
- 290 12. Dürig, T. *et al.* Particle shape analyzer Partisan - An open source tool for multi-standard two-  
291 dimensional particle morphometry analysis. *Annals of Geophysics* **61**, (2018).
- 292 13. Nurfiani, D. & Bouvet de Maisonneuve, C. Furthering the investigation of eruption styles  
293 through quantitative shape analyses of volcanic ash particles. *Journal of Volcanology and*  
294 *Geothermal Research* **354**, 102–114 (2018).
- 295 14. Haralick, R. M., Dinstein, I. & Shanmugam, K. Textural Features for Image Classification. *IEEE*  
296 *Trans Syst Man Cybern* **SMC-3**, 610–621 (1973).
- 297 15. D’Oriano, C. *et al.* Syn-Eruptive Processes During the January–February 2019 Ash-Rich  
298 Emissions Cycle at Mt. Etna (Italy): Implications for Petrological Monitoring of Volcanic Ash.  
299 *Front Earth Sci (Lausanne)* **10**, (2022).

- 300 16. D’Oriano, C., Bertagnini, A., Cioni, R. & Pompilio, M. Identifying recycled ash in basaltic  
301 eruptions. *Sci Rep* **4**, (2014).
- 302 17. Global Volcanism Program, 2024. [Database] Volcanoes of the World (v. 5.2.2; 22 Aug 2024).  
303 Distributed by Smithsonian Institution, compiled by Venzke, E.  
304 <https://doi.org/10.5479/si.GVP.VOTW5-2024.5.2>. (2024).
- 305 18. D’Oriano, C., Pompilio, M., Bertagnini, A., Cioni, R. & Pichavant, M. Effects of experimental  
306 reheating of natural basaltic ash at different temperatures and redox conditions. *Contributions*  
307 *to Mineralogy and Petrology* **165**, 863–883 (2013).
- 308 19. Benet, D., Costa, F., Pedreros, G. & Cardona, C. The volcanic ash record of shallow magma  
309 intrusion and dome emplacement at Nevados de Chillán Volcanic complex, Chile. *Journal of*  
310 *Volcanology and Geothermal Research* **417**, (2021).
- 311 20. Natural Earth. 2023. ‘Admin 0 - Countries.’ 1:10m scale. Natural Earth. Accessed August 19,  
312 2024. [https://www.naturalearthdata.com/downloads/10m-cultural-vectors/10m-admin-0-](https://www.naturalearthdata.com/downloads/10m-cultural-vectors/10m-admin-0-countries/)  
313 [countries/](https://www.naturalearthdata.com/downloads/10m-cultural-vectors/10m-admin-0-countries/). earth\_map\_ref. (2023).
- 314 21. Romero, J. E. *et al.* The initial phase of the 2021 Cumbre Vieja ridge eruption (Canary Islands):  
315 Products and dynamics controlling edifice growth and collapse. **431**, (2022).
- 316 22. Utami, S. B., Costa, F., Lesage, P. H., Allard, P. & Humaida, H. Fluid fluxing and accumulation  
317 drive decadal and short-lived explosive basaltic andesite eruptions preceded by limited  
318 volcanic unrest. *Journal of Petrology* **62**, 1–29 (2021).
- 319 23. Gertisser, R. *et al.* Geological History, Chronology and Magmatic Evolution of Merapi. in *Active*  
320 *Volcanoes of the World* 137–193 (Springer Science and Business Media Deutschland GmbH,  
321 2023). doi:10.1007/978-3-031-15040-1\_6.
- 322 24. Metcalfe, A. *et al.* Magmatic Processes at La Soufrière de Guadeloupe: Insights From Crystal  
323 Studies and Diffusion Timescales for Eruption Onset. *Front Earth Sci (Lausanne)* **9**, (2021).
- 324 25. Dixon, H. J. *et al.* The geology of Nevados de Chillan volcano, Chile. *Revista Geologica de Chile*  
325 **26**, 227–253 (1999).
- 326 26. Miyagi, I., Geshi, N., Hamasaki, S., Oikawa, T. & Tomiya, A. Heat source of the 2014  
327 phreatic eruption of Mount Ontake, Japan. *Bull Volcanol* **82**, (2020).
- 328 27. Bernard, A. *et al.* *Petrology and Geochemistry of the 1991 Eruption Products of Mount*  
329 *Pinatubo. Fire and mud; eruptions and lahars of Mount Pinatubo, Philippines* (1996).
- 330 28. Scheidegger, K. F., Federman, A. N. & Tallman, A. M. Compositional heterogeneity of tephra  
331 from the 1980 eruptions of Mount St. Helens. *J Geophys Res Solid Earth* **87**, 10861–10881  
332 (1982).
- 333 29. Nurfiani, D. *et al.* Combining Petrology and Seismology to Unravel the Plumbing System of a  
334 Typical Arc Volcano: An Example From Marapi, West Sumatra, Indonesia. *Geochemistry,*  
335 *Geophysics, Geosystems* **22**, (2021).
- 336 30. Chesner, C. A. & Rose, W. I. *Vol a Olo Stratigraphy of the Toba Tuffs and the Evolution of the*  
337 *Toba Caldera Complex, Sumatra, Indonesia*. vol. 53 (1991).
- 338